TORSION PENDULUM: THE MECHANICAL NONLINEAR OSCILLATOR

Samo Lasič, Gorazd Planinšič, *, Faculty of Mathematics and Physics University of Ljubljana, Slovenija*
Giacomo Torzo, *Department of Physics, University of Padova, Italy*

1. Introduction: applicability of the didactical apparatus

The main purpose of talking about nonlinear phenomena in school is to gain the students ability for distinguishing the nonlinear system from the linear one by qualitative observations of the system dynamics. The complex and qualitatively different behavior of nonlinear systems should be pointed out as an remarkable consequence of non-linearity that happens to occur very often in natural systems. Formal thinking plays an essential roll when basic features of a nonlinear system and its dynamics are compared to the linear system. A qualitative approach is particularly fruitful for developing the basic idea of the phenomena and gaining a deeper understanding of both linear and nonlinear systems.
The simplest example of nonlinear oscillator is the physical pendulum. The torsion pendulum [1, 2, 3] instead is considered as a didactical example of a nonlinear system that performs all the basic features of a dynamical system. According to the equation of motion the torsion pendulum is characterized as a Duffing oscillator. The Duffing equation is often numerically solved to analyze its dynamics [4, 5]. There are also known electric circuits that behave according to the Duffing equation [6]. Such systems are very precise and easy to analyze but they are abstract and hard to use for developing formal thinking.
The basic idea has been initiated and first experiments performed by prof. dr. Giacomo Torzo at University of Padua. The theoretical analysis as well as design and construction of improved apparatus has been done at Physics Department, University of Ljubljana as BSc thesis [7].
The apparatus can be used as a didactical tool for demonstrating:

- the amplitude dependence of the period of oscillation,
- the hysteresis phenomena in the response of sinusoidaly driven pendulum and
- bifurcation of stable orbits and the transition to chaotic motion.

Our construction is based on theoretical predictions and numerical simulations. The goal was to build a mechanical oscillator of large dimensions that would help the observer to recognize and understand the phenomena. The main problem was to find the design that will optimize the requirements mentioned above. For this reason we have chosen the construction that leaves all the free parameters to be varied to some extend.

2. Description of the apparatus

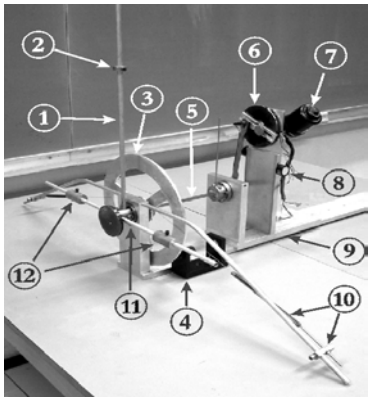

Building parts:

1. Oscillatory rod
2. Mass
3. Damping disk
4. Damping magnet
5. Steel tape
6. Driver with adjustable eccentric arm
7. Windscreen wiper motor
8. Buzzer
9. Movable bench
10. Spring for fine adjustment of zero angle
11. The pendulum head
12. Inertia rod with variable moment of inertia

Fig. 1: Vertical torsion pendulum

The oscillatory part of the pendulum consists of a weighted rod (Fig. 1 – part 1, part 2) fixed in the pendulum head (Fig. 1 – part 11) together with inertia rod with two symmetrically placed weights (Fig. 1 – part 12). The weights can be fixed on different positions enabling the center of mass and the moment of inertia to be changed respectively. The pendulum rod can be fixed either in the direction upward or downward. In this way two types of nonlinear restoring force can be achieved.
The driving mechanism consists of a windscreen wiper motor (Fig. 1 – part 7) and the rotating disc with eccentric driving arm (Fig. 1 – part 6) which transforms the rotation in approximately sinusoidal oscillation. The amplitude of driving oscillation can be varied in the range from 0° to 45° by changing the eccentric fixing of the arm.
The excitation is transferred to the oscillatory part of the pendulum through torsion distortion of the steel tape (Fig. 1 – part 5). The driving mechanism and the fixing of the tape to the driving arm are fixed on a movable bench (Fig. 1 – part 9). This allows using tapes of different length l, enabling one to change the tape torsion coefficient which is proportional to l^{-1}.
The viscose damping can be applied by bringing the magnet close to the 4 mm thick aluminum disc (Fig. 1 – part 3, part 4).
The fine adjustment of the zero equilibrium angle has been done by using two symmetrically placed linear springs (Fig. 1 – part 10). attached to the strings that are winded around the pendulum head. Each spring is fixed on a screw in the support to allow independent tension adjustment. In addition the springs help to reduce the torque on the motor.
The buzzer (Fig. 1 – part 8) gives a sound signal once per driving cycle. This is an excellent remedy to help the observer following the phase difference between pendulum and the driving oscillation. The buzzer is particularly useful for observing the period doubling transition to chaos.

3. Mathematical model of the torsion pendulum

In order to design a pendulum that will satisfy the demonstration requirements one should carefully choose the parameters. So let's take a look at the torsion pendulum model.
If the oscillation of driven torsion pendulum is confined to moderate angles (smaller then say 30°) the motion may be accurately modeled by the Duffing equation [8]

$$\ddot{x} + c\dot{x} + \alpha x + \beta x^3 = F\cos(\omega t), \qquad (1)$$

where c is the damping, coefficients α and β determine the linear and nonlinear part of the restoring force and $F\cos(\omega t)$ is the forcing term.
The sign of the coefficient β depends on the direction of the restoring force and determines the character of the pendulum behavior. In case where the pendulum rod is fixed in downward position $\beta<0$ (regular torsion pendulum), while for the rod in the upward position $\beta>0$ (inverted torsion pendulum).
The remarkable difference between the two types of torsion pendulum is seen from the form of potential energy that determines equilibrium and stable equilibrium angles (Fig. 2). In the case of regular torsion pendulum (Fig. 2.a) the potential energy is of the form

$$U(\theta) = \frac{1}{2}k\theta^2 - mgR\cos\theta \qquad (2)$$

and in the case of inverted torsion pendulum (Fig. 2.b)

$$U(\theta) = \frac{1}{2}k\theta^2 + mgR\cos\theta, \qquad (3)$$

where k is the torsion coefficient, m is the mass at center of mass distance R and θ is the angle between the pendulum rod and a vertical line.

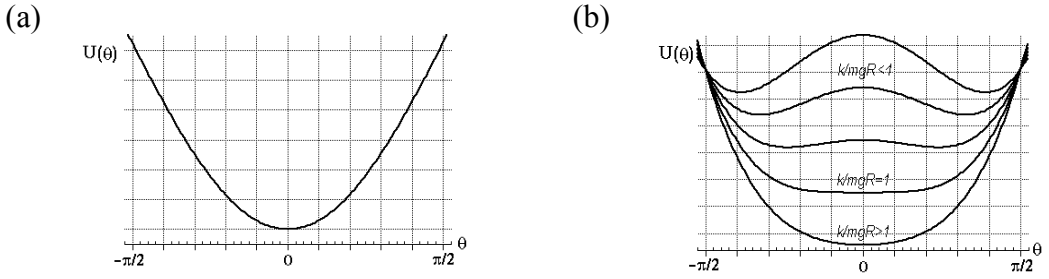

Fig. 2: Potential energy form in the case of regular torsion pendulum (a) and in the case of inverted torsion pendulum (b).

In the case of regular torsion pendulum the only equilibrium is a stable equilibrium at zero angle. In the case of inverted torsion pendulum instead we must consider two different situations. If the ratio $k/mgR>1$ there is only one stable equilibrium at zero angle similarly to the regular case. But for $k/mgR<1$ the zero equilibrium is a labile one. Beside this there are two symmetrically placed stable equilibrium angles

$$\theta_{\pm} = \pm\sqrt{6\left(1-\frac{k}{mgR}\right)}. \tag{4}$$

4. Period dependence on amplitude and the response to sinusoidal excitation

When the non-linearity is small the higher harmonics can be neglected and harmonic type of oscillation can be assumed. With this assumption we can calculate the period dependence on amplitude (Fig. 3) and the response to the sinusoidal excitation (Fig. 5).
To the first order in β the period dependence on amplitude is given by

$$\omega^2 = \alpha + \frac{3}{4}\beta A^2, \tag{5}$$

where ω is the circular frequency.

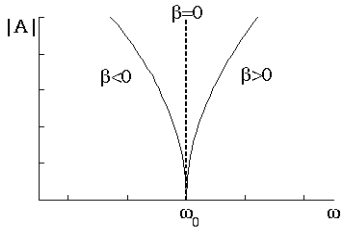

Fig. 3.: A schematic ω(A) diagram for free Duffing oscillator. The dashed line represents the harmonic oscillator.

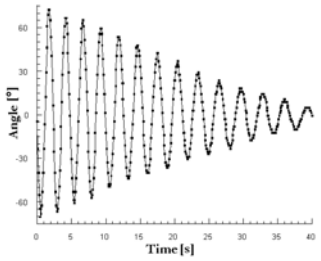

Fig. 4: Measured data for free oscillation of the inverted pendulum.

The period variation is particularly evident in the case of inverted pendulum where the period increases when the oscillation is damped (Fig. 4).
To calculate the response of the driven pendulum the Duffing iterative method is often used. The result can be written in the implicit form:

$$F^2 = \left[(\alpha-\omega^2)A + \frac{3}{4}\beta A^3\right]^2 + c^2\omega^2 A^2 \tag{6}$$

with the phase shift ϕ given by:

$$\tan\phi = \frac{c\omega}{\alpha - \omega^2 + 3/4\beta A^2}. \tag{7}$$

The response diagram shows the hysteresis phenomena. There is a region in the response diagram where two physical states of the system are possible. The resulting state depends on the initial conditions or on the value of the past driving frequency. When the driving frequency slowly increase the amplitude and phase jump occurs from point 1 to point 2 on the diagram but when the frequency decrease the jump occur from point 3 to point 4 (Fig. 5). To see the effect one must wait for transient oscillations to die out. The assumptions we took for the calculus of the response diagram seem realistic as the results (Fig. 6) confirm.

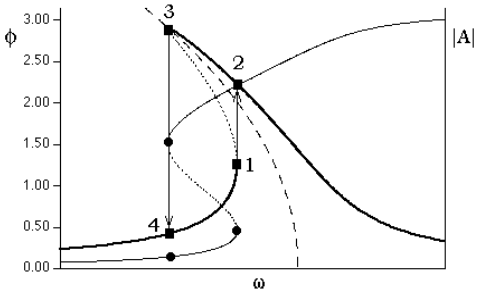

Fig. 5. The hysteresis in the response diagram for β<0. The jump occurs from point 1 to 2 when the driving frequency increases and from point 3 to 4 when the frequency decreases. The dashed line represents free oscillations. With the dotted line we marked the non-physical solution.

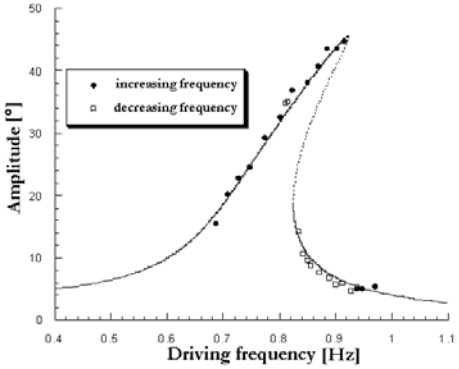

Fig. 6. Measured data confirm the hysteresis in the response diagram. Here is an example of inverted torsion pendulum (β>0).

5. The transition to chaos for inverted torsion pendulum

The complexity of the response increases with non-linearity. This is especially evident in the case of double potential energy well. The labile equilibrium at zero angle brings into the system the weak causality thus onsets the system for the chaotic motion. For some combinations of system parameters α, β, c, F, ω there is no periodicity and no evident order in the response oscillation. Choosing the parameters α and β which are determined by the pendulum dimensions one can change the damping c, the driving amplitude F or the driving frequency ω to enter the chaotic region. However, the transition to the chaotic region is gradual. Bifurcations of stable orbits follow the Feigenbaum scenario of period doubling finally reaching the chaotic motion.

With the didactical apparatus it is possible to vary any of the system parameters in order to achieve clear transition to chaos [4]. In our case the frequency can be easy adjusted by varying the voltage on the driving motor. We have chosen to enter the chaotic region by slowly decreasing the driving frequency. At relatively high frequencies the response repeats after one driving cycle (Fig. 7) what is usually called a one-period motion. If the frequency is gradually decreased one-period motion trajectory becomes unstable. The motion in phase diagram is now attracted to two different intersecting stable orbits. After one driving cycle the motion reaches the point of intersection and changes the orbit. In this case the response repeats after two driving cycles thus called a two-period motion (Fig. 8). The similar bifurcation phenomena with period doubling from two-period to four-period motion (Fig. 9) occurs when the frequency is further decreased. The driving frequency intervals from one doubling to another are geometrically decreasing and finally lead to the chaotic response (Fig. 10).

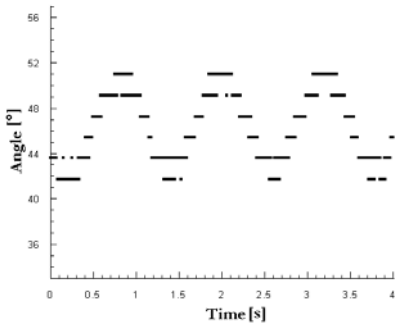

Fig. 7. Measured data: one-period motion (driving frequency ν=0,83 Hz).

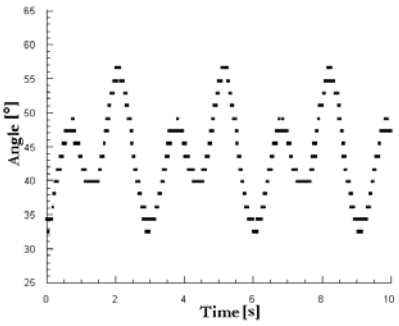

Fig. 8. Measured data: two-period motion (driving frequency ν=0,63 Hz).

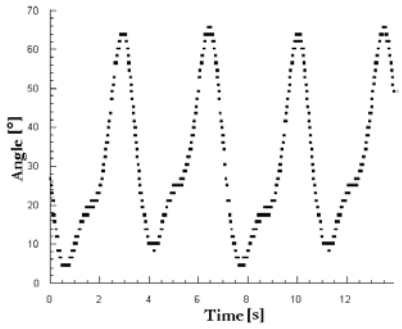

Fig. 9. Measured data: four-period motion (driving frequency ν=0,56 Hz).

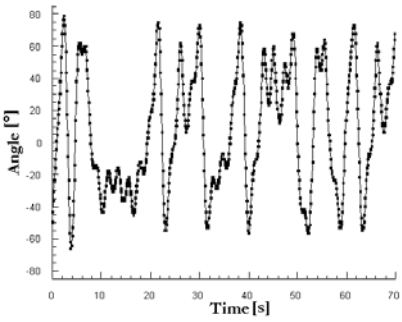

Fig. 10. Measured data: chaotic motion (driving frequency ν=0,47 Hz).

6. Conclusions

Experiments with the apparatus evidently confirm the theoretical predictions. The prototype can be used for developing an efficient didactical tool. The large dimensions result in slow and evident transients, easy observing the phase shift and the instability of periodic orbits in the transition to chaotic motion, thus making possible to gain a quality insight into the physical phenomena. With large dimensions the phenomena is fascinating, especially in the case of chaotic motion. However, too slow demonstrations are not efficient in classical lessons. For this reason the dimensions should be appropriately reduced.

References

[1] B. Duchesne, C. W. Fischer, C. G. Gray, K. R. Jeffrey, "Chaos in the motion of an inverted pendulum: An undergraduate laboratory experiment", *Am. J. Phys*., **59,** (1991), 987-992.
[2] C. L. Olson, M. G. Olsson, "Dynamical symmetry breaking and chaos in Duffing's equation", *Am. J. Phys*., **59,** (1991), 907-911.
[3] R. D. Peters, "Chaotic pendulum based on torsion and gravity in opposition", *Am. J. Phys*., **63,** (1995), 1128-1136.
[4] H. J. Korsch, *Chaos-a program collection for the PC*, Springer-Verlag, (1994).
[5] Internet pages for non-linear systems with simulations:
www.mcasco.com/pattr1.html.
www.apmaths.uwo.ca/~bfraser/version1/index.html.
www.chaos.engr.utk.edu.html,
http://monet.physik.unibas.ch/~elmer/pendulum/bif.htm.
[6] B. K. Jones, G. Trefan, "The Duffing oscillator: A precise electronic analog chaos demonstrator for the undergraduate laboratory", *Am. J. Phys*., **69,** (2001), 464-469.
[7] S. Lasič, The thesis work: "Didactical treatment of torsion pendulum with the transition to chaos", University of Ljubljana, Faculty for Mathematics and Physics, (2001).
[8] J. J. Stoker, *Nonlinear Vibrations in Mechanical and Electrical Systems,* Interscience Publishers, (1950).